

FIG. 1: (a) Schematic density of states of EuO. (b) Same for GdN. (c) Side view of proposed interface structure, comprised of one GdN layer atop one EuO layer on a SrO substrate. Large atoms are cations (Gd, Eu and Sr); small atoms are anions (N and O).

sults from our DFT calculations are then used as input to construct maximally-localized Wannier functions using WANNIER90 [29, 30]. Chern numbers and band gaps are calculated using Wannier interpolation of the band structure; the Chern numbers are computed by sampling the Brillouin zone (BZ) by a dense k -point grid and summing the Berry phases around the loops formed by each set of four adjacent k -points.

We begin by outlining our basic strategy for constructing a Chern insulator. Our goal is to find two topologically trivial materials that, when placed together, result in a band inversion and a Chern insulator. The (001) surface of EuO is nearly unique among binary compounds in providing a simple insulating non-polar surface that breaks time-reversal symmetry [31], making it a good starting point for our strategy. Both the valence and conduction bands of EuO consist of strongly spin-polarized bands localized on the Eu atom, as shown schematically in Fig. 1(a). Eu ($Z = 63$) provides strong SOC, making EuO an excellent candidate material. In fact, our calculations show that a single layer of EuO will become a Chern insulator under sufficiently strong compressive epitaxial strain, which reduces the band gap and eventually causes the conduction band to overlap with the valence band. Unfortunately, the strain necessary to cause this band inversion is unrealistically large ($\sim 10\%$), forcing us to look for a second material to combine with EuO to achieve the same effect under more realistic conditions. This second material should provide conduction bands of the correct symmetry such that they result in an avoided crossing and a transfer of Chern number when they overlap with the occupied Eu f states.

There are many candidate materials with the rock-salt structure that may be possible to interface epitaxially with EuO, but the majority of them are highly ionic materials with very large band gaps, making them unsuitable for this application. One exception is CdO, which has been studied previously in quantum wells and superlattices with EuO [32]. We find that this combination

does produce the desired Chern-insulating state for certain values of layer thickness and strain, but with a small band gap. The small gap results from the weak interaction between the Cd s and Eu f states near Γ , which can be understood in the context of the Wigner-Eckhart theorem, i.e., a first-order $\mathbf{k} \cdot \mathbf{p}$ perturbation ($\Delta l = 1$) cannot link $l = 0$ and $l = 3$ states, at least without assistance from the cubic crystal field ($\Delta l = 2$). In addition, the Cd s states have only a weak spin splitting arising from exchange coupling to the Eu; this results in a very limited phase space for non-trivial topological behavior before the Cd s state of opposite spin crosses the Fermi level and the system becomes metallic. Finally, CdO is poorly lattice-matched with EuO, which would make synthesis of these structures challenging.

Based on the example of CdO as well as general considerations of experimental feasibility, we conclude that the ideal rock-salt material to pair with EuO would have the following characteristics: 1) a similar lattice constant to EuO, 2) a large SOC, 3) a small band gap, 4) spin-polarized conduction bands with d -character, and 5) a conduction band minimum at Γ in the surface BZ. The only material we know of that meets all of these requirements is GdN, a ferromagnetic spin-polarized semi-metal in bulk which becomes insulating in thin-film form.

In Fig. 1(a-b) we present a schematic band-alignment diagram for GdN and EuO. We seek to engineer a band inversion between the Eu f state at the top of the valence band of EuO and the Gd $d_{x^2-y^2}$ orbital at the bottom of the conduction band of GdN by creating an interface between these two materials. In order to obtain the largest possible coupling between the two materials, we begin with single layers of EuO and GdN stacked on an SrO substrate, as shown in Fig. 1(c). We show the resulting surface band structure in Fig. 2, with all spins aligned ferromagnetically perpendicular to the surface, for two different values of in-plane lattice constant. At large lattice constants this interface is a trivial insulator, as shown in Fig. 2(a), but reducing the lattice constant to 3.53 \AA causes the band gap to close. At this critical strain, the Gd $d_{x^2-y^2}$ conduction-band minimum crosses the Eu $f_{x^3-iy^3}$ valence-band maximum at Γ . Further reduction of the lattice constant, as shown in Fig. 2(b), results in an avoided crossing and a transfer of Chern number from the valence band to the conduction band, leaving the occupied bands with a Chern number of -1 .

By varying the strain in the system, the band gap can be increased above 0.1 eV , as shown in the first three rows of Table I. This very robust gap can be traced to several factors. First, the atomically thin layers of GdN and EuO confine the relevant states at the interface, resulting in a large overlap. Second, as discussed above, the f and d character of the bands allows for first-order coupling between them. Finally, the large separation of the conduction-band minimum and valence-band maximum from other bands in the system allows for a large band

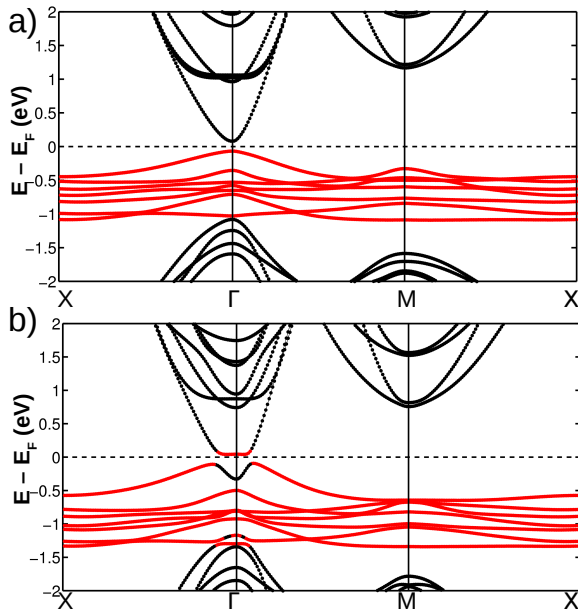


FIG. 2: Band structures of one GdN layer atop one EuO layer on an SrO substrate at (a) 3.62 Å ($C = 0$), and (b) 3.44 Å ($C = -1$). Majority Eu f states are plotted in red; others are in black.

N_{EuO}	N_{GdN}	a (Å)	C	E_g (meV)
1	1	3.62	0	111
1	1	3.53	-1	3
1	1	3.48	-1	130
2	1	3.62	-1	80
2	1	3.53	-1	123
1	2	3.48	-1	71
2	2	3.62	-1	62

TABLE I: Computed Chern number C and band gap E_g for N_{GdN} layers of GdN atop N_{EuO} layers of EuO on an SrO substrate of the specified lattice constant a .

inversion and a strong avoided crossing. This isolation of the relevant bands also allows for a relatively wide range of strains that can result in a Chern-insulating state, which should make our predictions more robust and easier to achieve experimentally.

The value of the Chern number in this system can be understood by examining the symmetries of the bands that take part in the avoided crossing [33]. At the Γ point of the BZ, the bands all belong to one of four non-degenerate irreducible representations that can be labeled by the eigenvalues of the four-fold rotation operator. In the case of a single band crossing where the eigenvalues of the bands differ only by a factor of $\pm i$, the exchange of Chern numbers is uniquely determined [34]. In the case of GdN on EuO, where the conduction-band minimum has the symmetry of a $d_{x^2-y^2}$ orbital, these

symmetry considerations imply that $C = -1$, consistent with our direct numerical calculations. In the case of CdO, the conduction band minimum has s -character, and $C = 1$.

In order to gain some insight into the behavior of this system, we build a simple two-band single-spin tight-binding model, in the spirit of the Haldane model [35], but here designed to capture the key behavior of the valence-band maximum and conduction-band minimum of our system. The model consists of a square lattice with a single $d_{x^2-y^2}$ orbital at $(0, 0)$ and a single $f_{x^3-iy^3}$ orbital at $(\frac{1}{2}, \frac{1}{2})$, labeled by $a = \{1, 2\}$. These orbitals have on-site energies $\pm\Delta$, and strong hoppings ($t_1 < 0, t_2 > 0$) to nearest neighbors of the same sublattice. The sublattices are coupled by a weaker complex interaction term, $\lambda_{ij} = u \hat{e}_{ij} \cdot (\hat{x} - i\hat{y})$, where u is the magnitude of the coupling and \hat{e}_{ij} is the direction of the hopping. This results in the Hamiltonian

$$H = \sum_{i,a} (-1)^{a+1} \Delta c_{ia}^\dagger c_{ia} + \sum_{\langle ij \rangle > a} t_a c_{ia}^\dagger c_{ja} + \sum_{\langle ij \rangle > a,b} \lambda_{ij} c_{ia}^\dagger c_{jb} + H.c. \quad (1)$$

The sums over i and j are over unit cells, and the sums over a and b are over the two orbitals. By reducing Δ , which mimics the impact of strain on the GdN/EuO system, the model can be tuned from a trivial to a Chern-insulating state, with the two phases separated by a band touching at Γ at the critical value of $\Delta_c = -2t_1 + 2t_2$. For Δ slightly below Δ_c , the band gap of the Chern insulating phase increases linearly with $\Delta_c - \Delta$, but for larger band inversions, the band gap of the Chern-insulating state begins to saturate, growing like $(\Delta_c - \Delta)^{\frac{1}{2}}$ as the avoided crossings move away from Γ . This behavior is consistent with our first-principles results showing increasing gaps for larger band inversions, as long as the two orbitals near the Fermi level remain separated from other bands in the system.

Returning to the first-principles results, we next consider thicker layers of both GdN and EuO. These thicker layers are likely to be easier to grow and measure experimentally, as well as more likely to have bulk-like magnetic ordering temperatures. First, we consider an additional GdN layer, as shown in Fig. 3(a). Consistent with our expectations, an additional layer of GdN results in a lower conduction-band minimum at a given lattice constant, consistent with the fact that thicker slabs of GdN should approach bulk-like semi-metallic behavior. This behavior is convenient because it allows the band structure to be tuned not only by strain, but also by varying the GdN layer thickness. We expect that as the GdN thickness increases, the relevant conduction-band state will become more delocalized, leading to less interaction with EuO and a smaller band gap. However, this effect appears to be fairly weak when going from one to two layers, as shown in Table I.

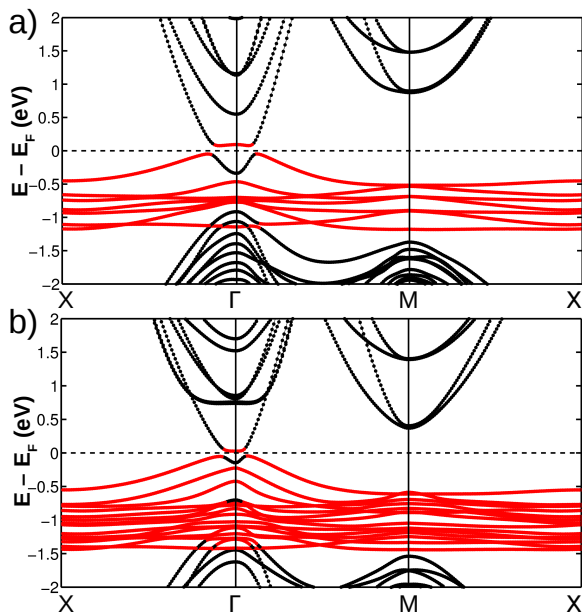


FIG. 3: Band structures of (a) two GdN layers atop one EuO layer on SrO at 3.53 Å, and (b) one GdN layer atop two EuO layers on SrO at 3.48 Å. Both have $C = -1$. Colors as in Fig. 2.

We also explore the band structure of a single GdN layer on top of two EuO layers, as shown in Fig. 3(b). This configuration also results in a Chern insulator for appropriate values of strain, but the additional Eu f levels from the second EuO layer limit the total band gap. This occurs because of the relatively weak splitting between the f orbitals on the two Eu atoms; for large band inversions, the $d_{x^2-y^2}$ band from the Gd crosses several of the Eu- f states, closing the band gap. However, as shown in Table I, the splitting between different Eu f levels is still large enough to allow significant band gaps, even for thicker EuO layers.

In all of the above calculations, we have assumed that the spins in both EuO and GdN align ferromagnetically, as they do in the bulk. As a preliminary test of this hypothesis, we consider an antiferromagnetic arrangement with a single spin-up GdN layer atop a single spin-down EuO layer on SrO at 3.53 Å, and we find that the antiferromagnetic configuration is 0.5 meV higher in energy than the ferromagnetic configuration considered previously. This energy difference is consistent, in sign and magnitude, with the calculated exchange parameters in bulk GdN and EuO [26, 27]. Further calculations would be needed to determine all of the relevant magnetic exchange parameters, as well as the effects of reduced dimensionality on the magnetic ordering temperature. In addition, we note that we have assumed that the spins align in the z direction; experimentally, this might require the application of a small external field. Nevertheless, with these qualifications, we believe the needed

magnetic structures should be attainable experimentally.

To summarize, our proposal results from a design strategy in which known topologically-trivial materials with strong spin-orbit coupling are combined in such a way as to engineer a band inversion, resulting in robust, topologically non-trivial behavior. We have shown that the (001) interface between GdN and EuO is an excellent candidate system for achieving a robust Chern-insulating state at temperatures of up to 70K and with band gaps of over 0.1 eV. This non-polar lattice-matched interface consists of known stoichiometric magnetic insulators, which should make it achievable experimentally.

Acknowledgments

This work was supported by NSF Grant DMR-10-05838.

-
- [1] C.-Z. Chang, J. Zhang, X. Feng, J. Shen, Z. Zhang, M. Guo, K. Li, Y. Ou, P. Wei, L.-L. Wang, et al., *Science* **340**, 167 (2013).
 - [2] F. Yang, Y. R. Song, H. Li, K. F. Zhang, X. Yao, C. Liu, D. Qian, C. L. Gao, and J.-F. Jia, *Phys. Rev. Lett.* **111**, 176802 (2013).
 - [3] S. Li, S. E. Harrison, Y. Huo, A. Pushp, H. T. Yuan, B. Zhou, A. J. Kellock, S. S. P. Parkin, Y.-L. Chen, T. Hesjedal, et al., *Applied Physics Letters* **102**, 242412 (2013).
 - [4] A. Kandala, A. Richardella, D. W. Rench, D. M. Zhang, T. C. Flanagan, and N. Samarth, *Applied Physics Letters* **103**, 202409 (2013).
 - [5] D. J. Thouless, M. Kohmoto, M. P. Nightingale, and M. den Nijs, *Phys. Rev. Lett.* **49**, 405 (1982).
 - [6] M. Z. Hasan and C. L. Kane, *Rev. Mod. Phys.* **82**, 3045 (2010).
 - [7] R. Yu, W. Zhang, H.-J. Zhang, S.-C. Zhang, X. Dai, and Z. Fang, *Science* **329**, 61 (2010).
 - [8] C.-X. Liu, X.-L. Qi, X. Dai, Z. Fang, and S.-C. Zhang, *Phys. Rev. Lett.* **101**, 146802 (2008).
 - [9] Z. Qiao, S. A. Yang, W. Feng, W.-K. Tse, J. Ding, Y. Yao, J. Wang, and Q. Niu, *Phys. Rev. B.* **82**, 161414 (2010).
 - [10] K. F. Garrity and D. Vanderbilt, *Phys. Rev. Lett.* **110**, 116802 (2013).
 - [11] A. Mauger and C. Godart, *Phys. Rep.* **141**, 51 (1986).
 - [12] U. Rossler and D. Strauch, *Group IV Elements, IV-IV and III-V Compounds, Group III Condensed Matter*, vol. 41A1a (Springer-Verlag, Berlin, 2001).
 - [13] P. Wachter and E. Kaldis, *Solid State Commun.* **34**, 241 (1980).
 - [14] J. Q. Xiao and C. L. Chien, *Phys. Rev. Lett.* **76**, 1727 (1996).
 - [15] P. Wachter, *Crit. Rev. Solid State Sci.* **3**, 198 (1972).
 - [16] P. Hohenberg and W. Kohn, *Phys. Rev.* **136**, B864 (1964).
 - [17] W. Kohn and L. Sham, *Phys. Rev.* **140**, A1133 (1965).
 - [18] G. Kresse and J. Hafner, *Phys. Rev. B* **47**, R558 (1993).
 - [19] G. Kresse and J. Furthmuller, *Phys. Rev. B* **54**, 11169 (1996).

- [20] P. E. Blöchl, Phys. Rev. B **50**, 17953 (1994).
- [21] G. Kresse and D. Joubert, Phys. Rev. B **59**, 1758 (1999).
- [22] J. P. Perdew, K. Burke, and M. Ernzerhof, Phys. Rev. Lett. **77**, 3865 (1996).
- [23] V. I. Anisimov, J. Zaanen, and O. K. Andersen, Phys. Rev. B **44**, 943 (1991).
- [24] S. L. Dudarev, G. A. Botton, S. Y. Savrasov, C. J. Humphreys, and A. P. Sutton, Phys. Rev. B **57**, 1505 (1998).
- [25] J. Heyd, G. E. Scuseria, and M. Ernzerhof, J. Chem. Phys. **118**, 8207 (2003).
- [26] M. Schlipf, M. Betzinger, M. Lezaic, C. Friedrich, and S. Blugel, Phys. Rev. B **88**, 094433 (2013).
- [27] M. Schlipf, M. Betzinger, C. Friedrich, M. Lezaic, and S. Blugel, Phys. Rev. B. **84**, 125142 (2011).
- [28] Unlike PBE0, HSE underestimates the EuO band gap, but in testing we found that calculations with PBE0 and HSE give very similar results near the Fermi level for GdN/EuO interfaces.
- [29] A. A. Mostofi, J. R. Yates, Y.-S. Lee, I. Souza, D. Vanderbilt, and N. Marzari, Comput. Phys. Commun. **178**, 685 (2008).
- [30] A. A. Mostofi, J. R. Yates, Y.-S. Lee, I. Souza, D. Vanderbilt, and N. Marzari, Comput. Phys. Commun. **178**, 685 (2008).
- [31] N. A. Spaldin, *Magnetic Materials* (Cambridge University Press, 2010).
- [32] H. Zhang, J. Wang, G. Xu, Y. Xu, and S.-C. Zhang, Phys. Rev. Lett. **112**, 096804 (2014).
- [33] J. Bellissard, arXiv:cond-mat/9504030 (1995).
- [34] C. Fang, M. J. Gilbert, X. Dai, and B. A. Bernevig, Phys. Rev. Lett. **108**, 266802 (2012).
- [35] F. D. M. Haldane, Phys. Rev. Lett. **61**, 2015 (1988).